Pakistan Journal of Applied Sciences 1 (3): 275-282, 2001

Numerical Simulation of Low Reynolds Number Flows in In-Line Tube Banks

E. Shirani and H. Nasibi
Department of Mechanical Engineering, Isfahan University of Technology, Isfahan, Iran

Abstract: A body fitted curvilinear coordinate system is incorporated with Beam-Warming numerical method to solve full Navier-Stokes and energy equations for laminar flow of air around three isothermal horizontal cylinders in an in-line tube bank. The effects of longitudinal and transverse pitches and Reynolds number ranged from 25 to 2500 on the flow parameters such as streamlines, surface pressure, total drag, pressure drag and friction drag coefficients, and hydraulic drag around tube banks are considered. The change of longitudinal and transverse pitches and the Reynolds number affects the flow parameters. As longitudinal pitch is decreased, the wakes behind the cylinders are spread between two rows. There is an optimum value for longitudinal pitch, at which, the hydraulic drag is minimum. The drag coefficient decreases as Reynolds number increased or as the transverse pitch increased.

Keywords: In-line Tube Banks, Heat Transfer, Flow Characteristics

Introduction

The study of flow normal to a bank of tubes continues to attract interest because of its importance in heat exchangers design. Related engineering applications of the heat transfer and flow characteristics of tubes in staggered or in-line tube banks have been presented by many researchers. Zhukauskas (1987) studied the heat transfer from tubes in cross flow. Launder and Massey (1978) presented their numerical prediction of viscous flow and heat transfer in tube banks. Chen and Wong (1986) investigated flow around three tube arrangements. Martin, et al (1998) investigated heat transfer and fluid friction in flow across banks of tubes. Gowda and Narayana (1998) presented a numerical analysis of laminar flow and heat transfer in in-line tube banks. Chang, Lai and Liu (1998) have investigated the thermal-hydraulic characteristics of circular finned-staggered tube banks.

In this work, flow characteristics around three cylinders as in-line tube banks are simulated numerically. For range of Reynolds number considered in this work, there were no appropriate experimental or numerical results to compare with. So our computer code and results were verified first by using available results for flow across a single cylinder.

Problem Description and Equations: Consider three isothermal heated horizontal cylinders as shown in Fig. 1. The fluid is air and the flow is assumed to be steady and two-dimensional. Based on the symmetry, only one part of arrays is needed for the solution of flow field, as shown in Fig. 1.

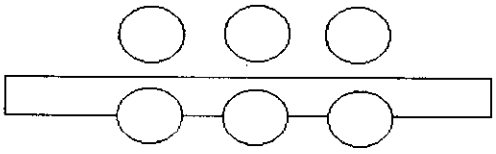

Fig. 1: Computational domain for in-line arrangement

The Cartesian velocity components are retained as dependent variables and two-dimensional, unsteady Navier-Stokes equations are transferred to an arbitrary curvilinear space, ξ, η, τ, as shown in Fig. 2.

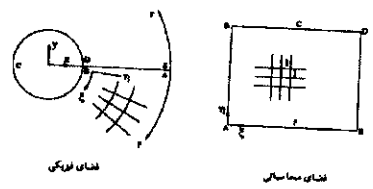

Physical space Computational space

Fig. 2: Body and Transformation coordinate

The resulting equations, which are in strong conservation form, can be written in non-dimensional form as Pulliam and Steger (1980):

$$\partial_\tau \hat{Q} + \partial_\xi \hat{E} + \partial_\eta \hat{F} = Re^{-1}(\partial_\xi \hat{E}_v + \partial_\eta \hat{F}_v) \quad (1)$$

where

$$\hat{Q} = J^{-1}\begin{bmatrix}\rho\\ \rho u\\ \rho v\\ e\end{bmatrix};\ \hat{E} = J^{-1}\begin{bmatrix}\rho U\\ \rho u U + \xi_x p\\ \rho v U + \xi_y p\\ U(e+p) - \xi_t p\end{bmatrix};\ \hat{F} = J^{-1}\begin{bmatrix}\rho V\\ \rho u V + \eta_x p\\ \rho v V + \eta_y p\\ V(e+p) - \eta_t p\end{bmatrix} \quad (2)$$

where U and V are contravariant velocities and given by:

$$U = \xi_t + \xi_x u + \xi_y v$$
$$V = \eta_t + \eta_x u + \eta_y v \quad (3)$$

The viscous flux terms are given by:

$$\hat{E}_v = J^{-1}\begin{bmatrix} 0 \\ \xi_x \tau_{xx} + \xi_y \tau_{xy} \\ \xi_x \tau_{yx} + \xi_y \tau_{yy} \\ \xi_x f_4 + \xi_y g_4 \end{bmatrix} \quad ; \quad \hat{F}_v = J^{-1}\begin{bmatrix} 0 \\ \eta_x \tau_{xx} + \eta_y \tau_{xy} \\ \eta_x \tau_{yx} + \eta_y \tau_{yy} \\ \eta_x f_4 + \eta_y g_4 \end{bmatrix} \qquad (4)$$

and

$$\begin{aligned} \tau_{xx} &= \mu\left[4\left(\xi_x u_\xi + \eta_x u_\eta\right) - 2\left(\xi_y v_\xi + \eta_y v_\eta\right)\right]/3 \\ \tau_{xy} &= \mu\left[\xi_x v_\xi + \xi_y u_\xi + \eta_y u_\eta + \eta_x v_\eta\right] \\ \tau_{yy} &= \mu\left[-2\left(\xi_x u_\xi + \eta_x u_\eta\right) + 4\left(\xi_y v_\xi + \eta_y v_\eta\right)\right]/3 \\ f_4 &= u\tau_{xx} + v\tau_{xy} + \mu \Pr^{-1}(\gamma-1)^{-1}\left(\xi_x \partial_\xi a^2 + \eta_x \partial_\eta a^2\right) \\ g_4 &= u\tau_{xy} + v\tau_{yy} + \mu \Pr^{-1}(\gamma-1)^{-1}\left(\xi_y \partial_\xi a^2 + \eta_y \partial_\eta a^2\right) \end{aligned} \qquad (5)$$

Pressure is denote as:

$$p = (\gamma - 1)\left[e - \frac{1}{2}\rho\left(u^2 + v^2\right)\right] \qquad (6)$$

where γ is the specific heat ratio, the metrics are:

$$\xi_x = J y_\eta \quad ; \quad \xi_y = -J x_\eta \quad ; \quad \xi_t = -x_\tau \xi_x - y_\tau \xi_y$$
$$\eta_x = -J y_\xi \qquad \eta_y = J x_\xi \qquad \eta_t = -x_\tau \eta_x - y_\tau \eta_y \qquad (7)$$

and J is the Jacobian of the coordinate transformation. Along the boundaries of the lower and upper symmetric planes, the gradient of all parameters are set to be zero. Along the cylinders' surface, the no slip conditions are applied. Since the flow is subsonic, the inflow requires three parameters and the outflow requires one parameter. So that at the inflow boundary condition, ρ, u and v are given and p is interpolated. At the outflow condition, p is specified and other parameters are interpolated. The free stream conditions applied as an initial condition in the flow field.

Numerical Method: The boundary fitted coordinate in which grid line coincides with the body surface is used. The partial differential equations proposed by Chen and Obasih (1986) are used to generate such a grid. These equations are:

$$\begin{aligned} a x_{\xi\xi} + c x_{\eta\eta} &= 0 \\ a y_{\xi\xi} + c y_{\eta\eta} &= 0 \end{aligned} \qquad (8)$$

where a and c are transformation coefficients:

$$a = x_\eta^{\,2} + y_\eta^{\,2} \quad ; \quad c = x_\xi^{\,2} + y_\xi^{\,2} \qquad (9)$$

J denotes the Jacobian of the transformation

$$J = \left(x_\xi y_\eta - x_\eta y_\xi\right)^{-1} \qquad (10)$$

and the control functions P and Q are

$$P(\xi,\eta) = -J^2\sqrt{ac}\left(\sqrt{\frac{a}{c}}\right)_\xi \qquad (11a)$$

$$Q(\xi,\eta) = J^2 c\left[J\left(y_\xi x_{\eta\eta} - x_\xi y_{\eta\eta}\right)\right]_{\Gamma_i} \qquad (11b)$$

The term with brackets in Eq. (11b) is evaluated at a boundary Γ_i. Fig. 3 shows the resulting grid generated Equations (1) have been solved by using a Beam-Warming (1976) non-iterative approximate factorization implicit scheme of the form

$$\begin{aligned} &[I + \Delta t \delta_\xi \hat{A}^n - D_i|_\xi][I + \Delta t \delta_\eta \hat{B}^n - \Delta t Re^{-1}\delta_\eta\left(J^{-1}\hat{M}^n\right) - D_i|_\eta]\Delta\hat{Q}^n = \\ &-\Delta t\left[\delta_\xi \hat{E}^n + \delta_\eta \hat{F}^n - Re^{-1}\delta_\eta \hat{S}^n\right] - D_e\hat{Q}^n \end{aligned} \qquad (12)$$

where δ is the typical central difference operator. The matrices $\hat{A}, \hat{B}$ and $\hat{M}$ result from local linearization about the previous time level. This equation is a block tridiagonal matrix type.

Since the central space difference operators are used, to prevent numerical oscillations, the second and forth order numerical dissipation terms denoted as Di and De respectively, have been added to Eq. (12).

$$D_e = h\varepsilon_e J^{-1}\left[\left(\nabla_\xi \Delta_\xi\right)^2 + \left(\nabla_\eta \Delta_\eta\right)^2\right]J \qquad (13)$$

$$D_{i|\xi} = J^{-1} h \varepsilon_i \nabla_\xi \Delta_\xi J \quad , \quad D_{i|\eta} = J^{-1} h \varepsilon_i \nabla_\eta \Delta_\eta j \qquad (14)$$

where ∇ and Δ are two-point backward and forward difference operators respectively, $\varepsilon_i > 2\varepsilon_e$ and $\varepsilon_e = O(1)$.

Results and Discussions

Flow Around a Single Cylinder: The available experimental results for flow around tube banks are only correspond to large numbers of rows (more than 10 rows) and high Reynolds number flows. So to examine the correctness of our numerical method, grid configuration and boundary conditions, flow around a cylinder were simulated first and compared with available results.

Fig. 4 shows the surface pressure coefficient along the circumference of the cylinder for Re=1.4E+5 and Ma=0.1. The results are compared with the experimental work done by Cantwell (1983). As shown, good agreements are obtained for the location of separation point and the location and value of minimum pressure.

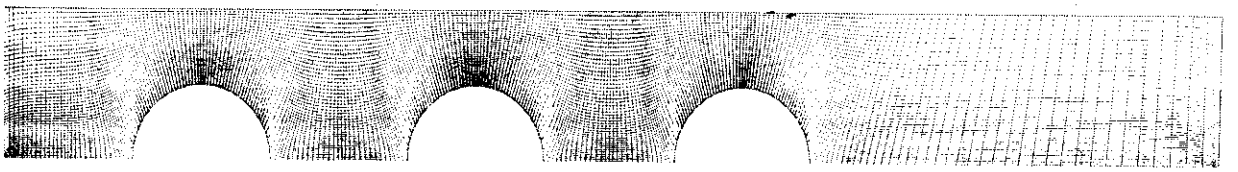

Fig. 3: Computational grid

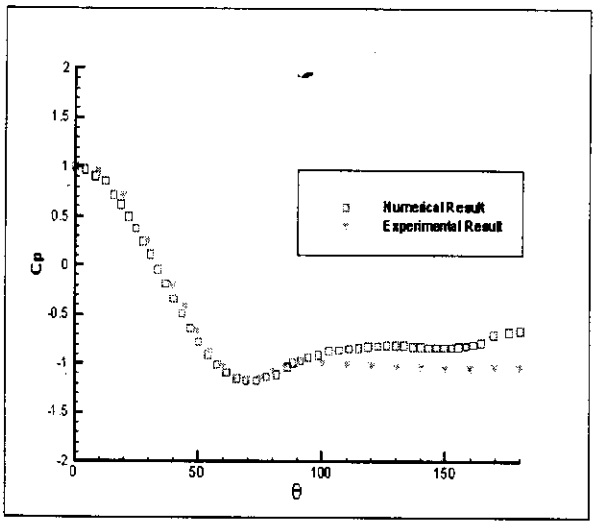

Fig. 4: Surface pressure coefficient along the cylinder body

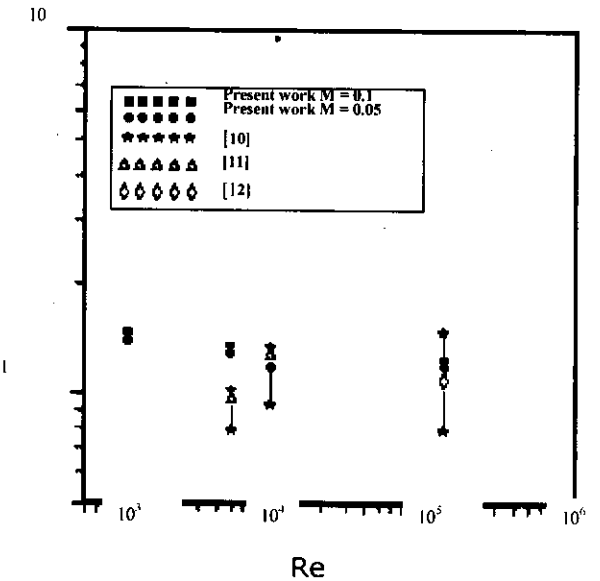

Fig. 5: Average drag coefficient as a function of Reynolds number

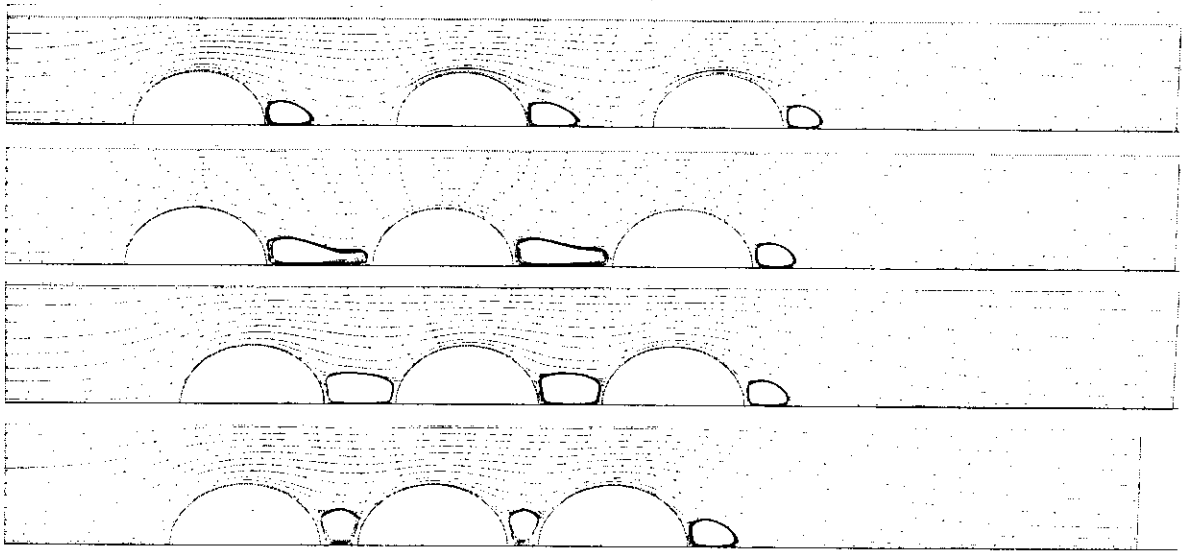

Fig. 6:Streamlines for differnt longitudinal pitch (a) 2d, (b) 1.75d , (c) 1.5d and (d) 1.25d

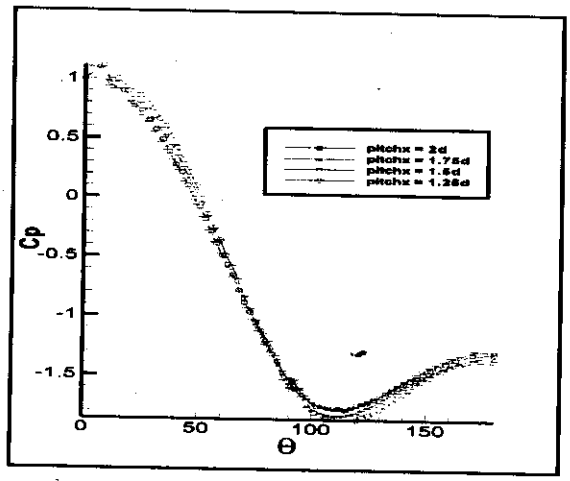

(a)

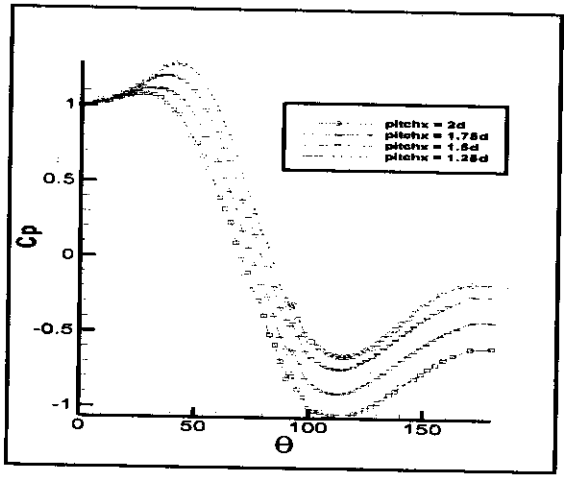

(b)

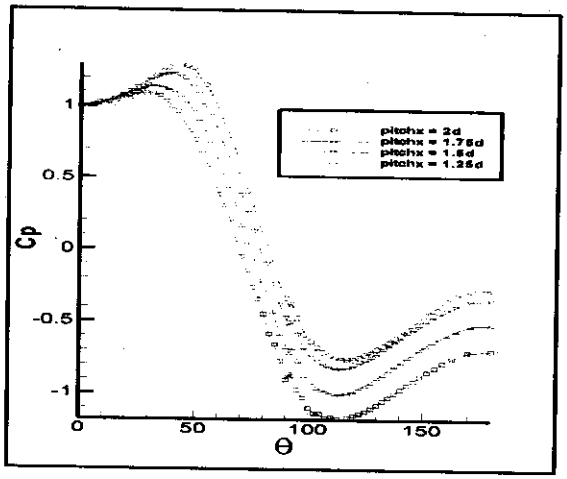

(c)

Fig. 7: Surface pressure coefficient distribution on (a) 1st row, (b) 2nd row and (c) 3rd row for different longitudinal pitches

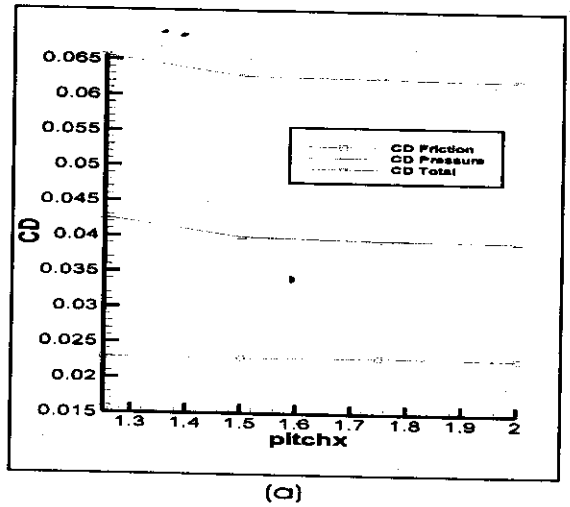

(a)

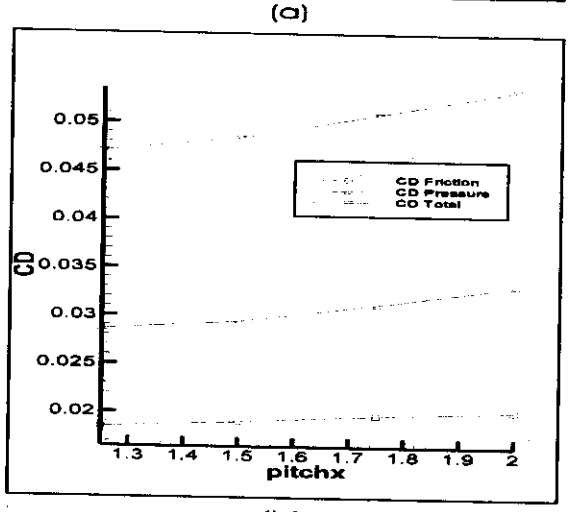

(b)

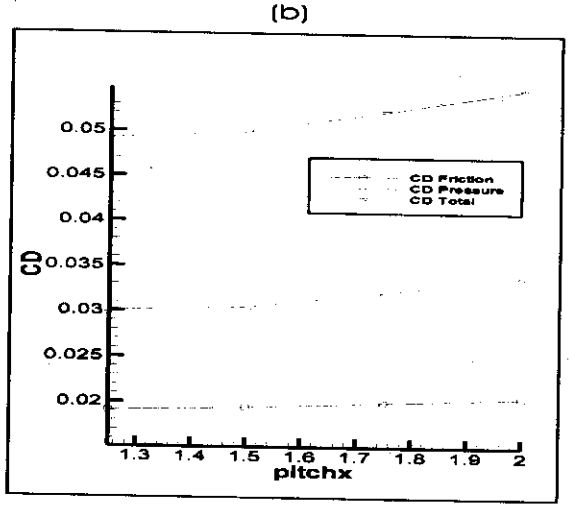

(c)

Fig. 8: Variation of total, pressure and friction drag coefficient on (a) 1st row, (b) 2nd row and (c) 3rd row for different longitudinal pitches

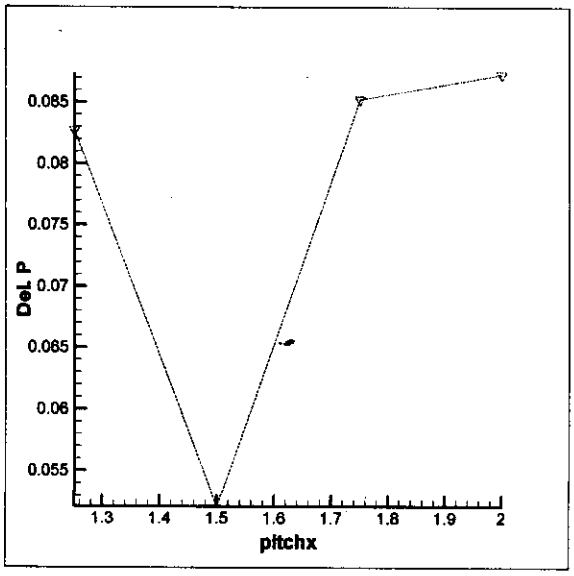

Fig. 9: Variation of the tube bank pressure drop with longitudinal pitch

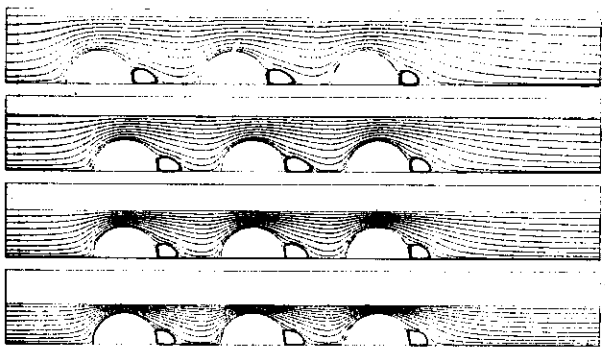

Fig. 10: Streamlines for different transverse pitch (a)2d, (b) 1.75d, (c) 1.5d and (d) 1.25d

Fig. 5 shows the average drag coefficient as a function of Reynolds number. In this Fig. the experimental results obtained by others are also shown. The results are well within the experimental results.

Numerical Results for Flow around a Tube Bank: In this section, the laminar flow of air around three isothermal cylinders in an in-line tube bank for different longitudinal and transverse pitches and Reynolds number ranged from 25 to 2500 are considered.

Longitudinal Pitch Study: The effects of longitudinal pitch on the flow parameters are considered. The transverse pitch, Reynolds and Mach numbers are 2.0d, 1000 and 0.1 respectively, where d is the cylinder diameter. The longitudinal pitch is varied from 1.25d to 2.0d.

Fig. 6 represents streamlines for the selected longitudinal pitches. As is shown, the recirculating zone or wake is generated behind the cylinders and with decreasing the longitudinal pitch, this wake is spread between two rows.

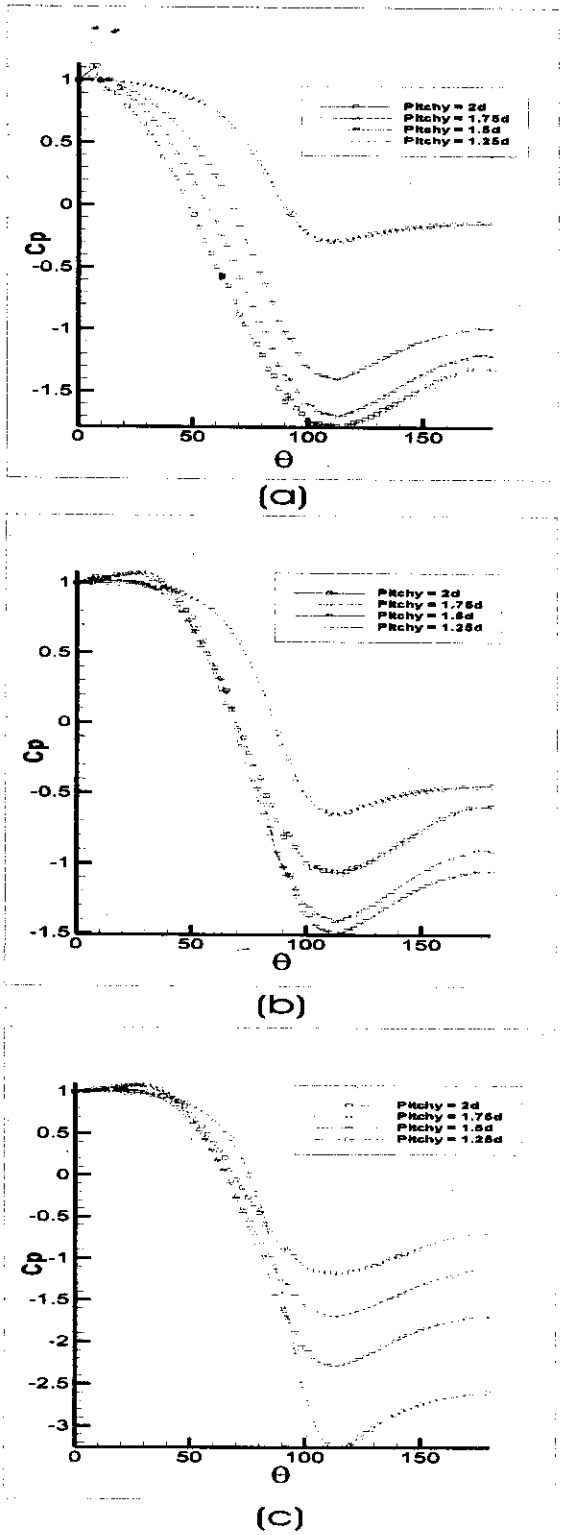

Fig. 11: Surface pressure coefficient distribution on (a) 1st row, (b) 2nd row and (c) 3rd row for different transverse pitches

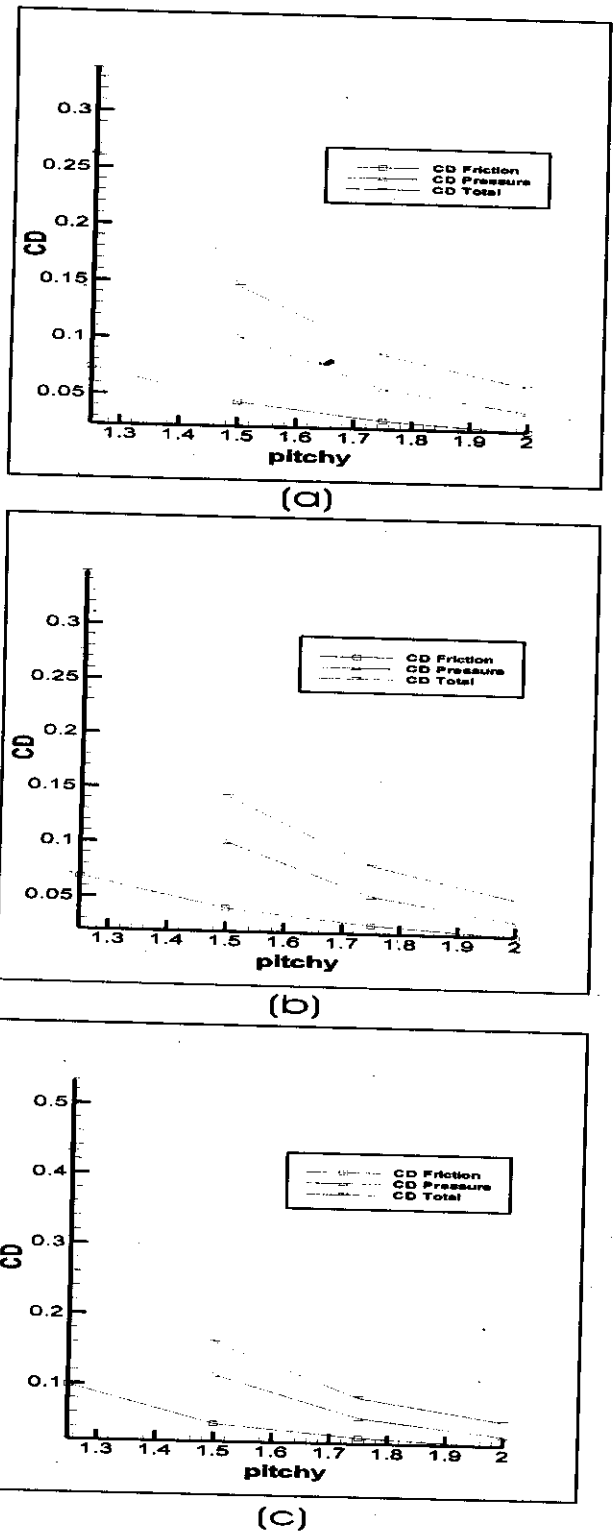

Fig. 12: Variation of total, pressure and friction drag coefficjent on 1st row, (b) 2nd row and (c) 3rd row for different transverse pitches

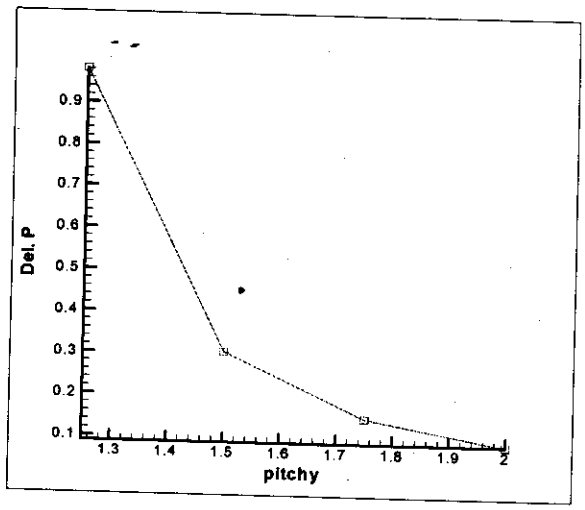

Fig. 13: Variation of the tube bank pressure drop with transverse pitch

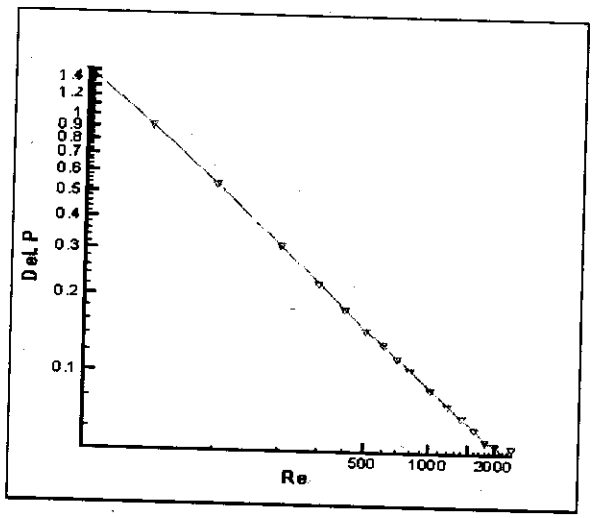

Fig. 14 Variation of the tube bank pressure drop with Reynolds number

The surface pressure coefficient distributions and the variations of total drag, pressure drag and friction drag coefficients are shown in Figs. 7 and 8 respectively. It is clear from these figures that the increase in longitudinal pitch causes a significant decrease of Cp and in the 2nd and 3rd rows but the variation at the 1st row is not as much.

The variation of pressure drop along the tube bank with longitudinal pitch is shown in Fig. 9. As shown, the optimum longitudinal pitch of the tube bank, which belongs to the minimum pressure drop case, is occurred where the longitudinal pitch is 1.5d.

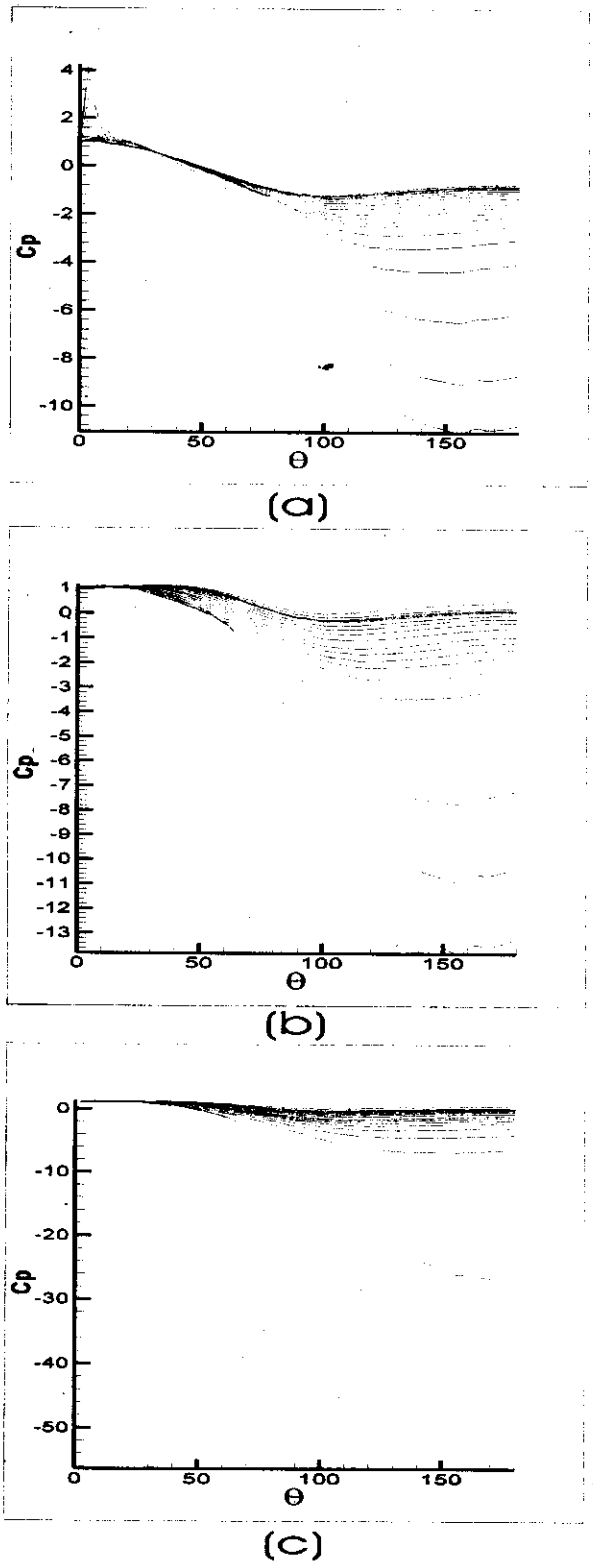

Fig. 15: Surface pressue coefficient distribution on 1st row, (b) 2nd row and (c) 3rd row for different Reynolds number

Transverse Pitch Study: The effects of transverse pitch on the flow parameters are considered. In this case longitudinal pitch, Reynolds and Mach numbers are 2.0d, 1000 and 0.1 respectively, where d is cylinder diameter. The transverse pitch is varied from 1.25d to 2.0d.

Fig. 10 represents streamlines for the selected longitudinal pitches. As shown, the recirculating zones or wakes, which are generated behind the cylinders, do not spread between rows as the transverse pitch decreases. The surface pressure coefficient distribution and the variations of total drag, pressure drag and friction drag coefficients are shown in Figs. 11 and 12 respectively. As shown in these figures, as transverse pitch increases, the drag coefficient in the 1st, 2nd and 3rd rows are decreased, but it effects differently on Cp from one row to nother.

The variation of tube bank pressure drag with longitudinal pitch is shown in Fig. 13. It is clear from this figure that as the transverse pitch decreases, the hydraulic drag of the tube bank is increased significantly.

Reynolds Number Study: The effects of Reynolds number on the flow and heat transfer parameters are considered. In this case longitudinal and transverse pitches and Mach number are 2.0d, 2.0d and 0.1 respectively, where d is the cylinder diameter and the Reynolds number is varied from 25 to 2500.

The variation of tube bank pressure drop with respect to Reynolds number based on logarithmic scale is shown in Fig. 14. It is shown that as Reynolds number increases, the hydraulic drag of tube bank decreases such that their log-log curve is linear.

The surface pressure coefficient distribution and the variations of total drag, pressure drag and friction drag coefficients with respect to Reynolds number based on logarithmic scale are shown in Figs. 15 and 16 respectively. It is clear from Fig. 15 that as Reynolds number increases, Cp would increase as expected. Fig. 16 illustrates that as the Reynolds number increases, C_D decreases.

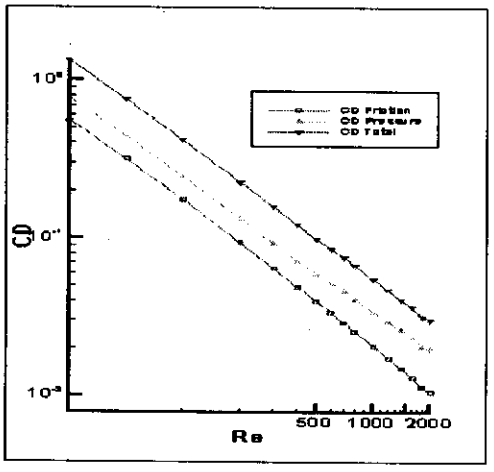

Fig. 16: (a)

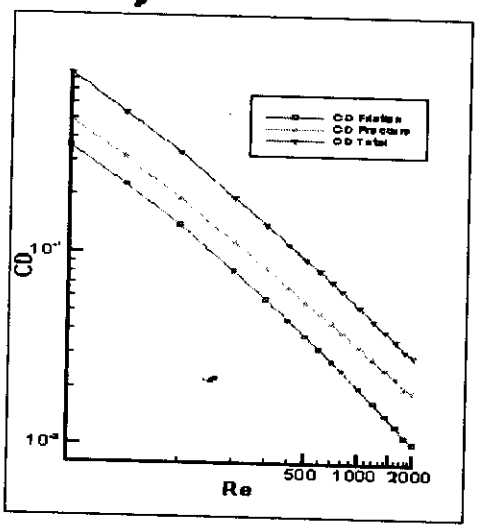

(b)

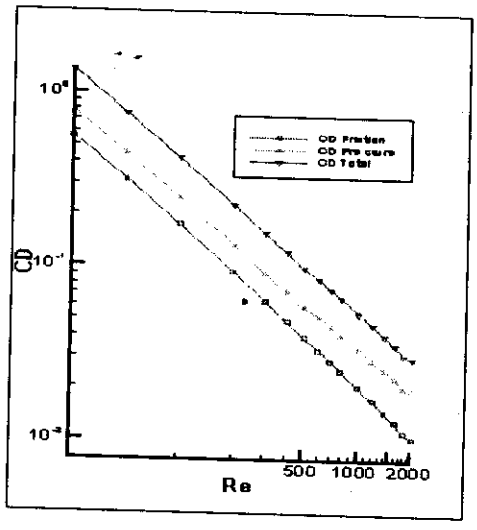

(c)

Fig. 16: Variation of total, pressure and friction drag coefficient in logarithmic scale on 1st row, (b) 2nd row and (c) 3rd row with Reynolds number

Conclusions

The change of longitudinal and transverse pitches and Reynolds number affects the flow and heat transfer parameters.

It is concluded that:

1. As longitudinal pitch is decreased, the wakes behind the cylinders are spread between two rows but as transverse pitch is decreased, the wakes do not spread between rows.
2. As longitudinal pitch is decreased, the hydraulic drag of tube bank is decreased first and then increased. The optimum longitudinal pitch of the bank, which belongs to the minimum hydraulic drag case, is 1.5d.
3. As transverse pitch is decreased, the hydraulic drag of tube bank is increased
4. The increase in longitudinal pitch causes a significant decrease of drag coefficient but the variation at the 1st row is not as much.
5. As transverse pitch increases, the drag coefficient in the 1st,2nd and 3rd rows are decreased.
6. As Reynolds number increases, the drag coefficient and hydraulic drag of tube bank are decreased logarithmically.

Notation

Cp Surface pressure coefficient

$$Cp = 1 - \frac{p_{\theta=0} - p}{\rho u_{max}^{\ 2}/2}$$

C_D	Drag Coefficient
Pitch x	Longitudinal Pitch
Pitch y	Transverse Pitch
d	Cylinders diameter
Re	Inflow Reynolds number based on cylinder diameter
Ma	Inflow Mach number

References

Beam, R., M. and R. F. Warming, 1976. "An Implicit Finite Difference Algorithm for Hyperbolic Systems in Conservation-Law-Form", J. Comp. Phys., 22: 87-110.

Cantwell, B. and D. Coles, 1983. "An Experimental Study of Entertainment and Transport in the Turbulent Near Wake of a Circular Cylinder", J. Fluid Mechanics, 136: 321-374.

Chen, C., K. Wong, 1986."Finite Element Solution of Laminar Flow and Heat Transfer of Air in a Staggered and In-Line Tube Bank", J. Heat & Fluid Flow, 7: 291-300.

Chen, C., J., and K. M. Obasih, 1986. "Numerical Generation of Nearly Orthogonal Boundary-Fitted Coordinate System", Proceeding, The Symposium on Advancement in Aerodynamics, Fluid Mechanics and Hydraulic, ASCE, Minneapolis, MN, PP 585-592.

Chang, J., J. Lai, L. Liu, 1998. "The Thermal-Hydraulic Characteristics of Staggered Circular Finned-Tube Heat Exchangers Under Dry and Dehumidifying Conditions", Int. J. Heat & Mass Transfer 41: 3321-3337.

Farell, C., J. Blessmann, 1983. "On Critical Flow Around Smooth Circular Cylinder", J. Fluid Mech. 136: 375-391.

Gowda, Y. and P. Narayana, 1998. "Finite Element Analysis of Mixed Convection Over In-Line Tube Bundle", Int. J. Heat & Mass Transfer, 41: 1613-1619.

Massy, T., B.Lounder, 1978."The Numerical Prediction of Viscous Flow and Heat Transfer in Tube Banks", J. Heat Transfer 100: 565-571.

Martin, A., C. Saltiel, and W. Shyy, 1998. "Frictional Losses and Convective Heat Transfer in Sparse, Periodic Cylinder Arrays in Cross Flow", Int. J. Heat & Mass Transfer, 41: 2383-2397.

Pulliam, T., and J. Steger, 1980 "Implicit Finite Difference Simulation of Three-Dimensional Compressible Flow", AIAA J. 18: 159-167.

Song, Charles, C. S. and M. Yuan, 1990. "Simulation of vortex shedding flow about a cylinder at high Reynolds numbers ", J. Fluids Engineering, 112: 155-163.

Zukauskas, A. 1987."Heat Transfer From Tubes in Crossflow", Advanced in Heat Transfer, 18: 87-159.